Development of Ti/Ti-DLC multilayers on magnesium alloys — Part 2: Corrosion and wear resistance

Wenling Xie [a,b], Cuixia Guo [b], Yiman Zhao [d], Lin Chen [a,*], Bin Liao [e], Sam Zhang [c,*]

[a] Laboratory of Beam Technology and Energy Materials, Advanced Institute of Natural Sciences, Beijing Normal University at Zhuhai, Zhuhai 519087, China
[b] School of Mechanical Engineering, Sichuan University of Science and Engineering, Zigong 643000, China
[c] Centre for Advanced Thin Films and Devices, School of Materials and Energy, Southwest University, Chongqing 400715, China
[d] School of Intelligent Manufacturing, Luoyang Institute of Science and Technology, Luoyang 471023, China
[e] School of Nuclear Science and Technology, Beijing Normal University, Beijing 100875, China

ARTICLE INFO

ABSTRACT

To improve corrosion and wear resistance of magnesium alloy, the Ti-DLC monolayer and Ti/Ti-DLC multilayer films were deposited on AZ31 magnesium alloys by filter cathodic vacuum arc deposition technology. All coatings showed good corrosion and wear resistance, and low friction coefficient. The corrosion resistance of the coated samples, from high to low, was Ti/Ti-DLC)2 multi coated-, Ti-DLC mono coated-, and Ti/Ti-DLC)4 multi coated samples. That is because the good toughness and film/substrate deformation coordination of multilayer films were beneficial for improving the corrosion resistance of coating, but the thinner Ti sublayer increased the risk of corrosion liquid penetrating the coating. Under friction test under 5 N load for 30 min, the Ti-DLC monolayer film showed best wear resistance with lowest wear rate as its combination effects of high hardness and good toughness. Whereas, under higher load, the higher toughness and film/substrate deformation coordination of multilayer films played a more positive role in its wear life. Under load of 10 N, comparing to the Ti-DLC monolayer film, the (Ti/Ti-DLC)4 multi and (Ti/Ti-DLC)2 multi films improved wear life by 15 % and 36 %, respectively. The (Ti/Ti-DLC)2 multi film had the best corrosion resistance and wear life.

1. Introduction

Compared with other metals such as aluminum alloy, titanium alloy, and stainless steel, magnesium alloy has poor wear and corrosion resistance [1,2], which hinders the application of magnesium alloy. Composition purification [3,4], alloying [5], and surface modification [6,7] etc. have been applied to solve this problem. Among them, surface modification, such as coating [8,9], can economically guarantee the practical application needs of magnesium alloy and maintain its light-weight advantage. Diamond like carbon (DLC) film is a kind of amorphous carbon film similar to diamond, has good corrosion resistance [10]. In addition, DLC film has good wear resistance due to its good lubricity, low friction coefficient, and the transfer film formed on the grinding ball.

H. Cao et al. [11] prepared the Ti/Ti-DLC (Ti doped DLC) bilayer films on the aluminum alloys by filter cathodic vacuum arc (FCVA) deposition. Metal doping can reduce residual stress [12,13], improve adhesion, and avoid DLC film peeling off from the substrate. By

extending corrosion channels [14–16] and suppressing crack initiation and propagation [17,18] during friction and wear processes through multiple interface effects, multilayer structure is beneficial for improving corrosion and wear resistance. In addition, FCVA deposition can prepare coatings with high adhesion and dense structure on various substrates, even temperature sensitive magnesium alloy substrates [16,17,19]. Therefore, the Ti/Ti-DLC multilayer films prepared by FCVA deposition technology are expected to improve both corrosion resistance and wear resistance of magnesium alloy.

In Part I, the Ti-DLC monolayer and Ti/Ti-DLC multilayer films prepared by FCVA showed compact structure and good adhesion strength. And the transition layer composed of Ti adhesive layer/Ti-DLC insulating layer/Ti interlayer was used to reduce the galvanic corrosion between Ti sublayer and magnesium alloy. In Part 2, the corrosion and wear resistance of Ti-DLC monolayer and Ti/Ti-DLC multilayer films, and improvement mechanism of corrosion and wear resistance were discussed.

Table 1

Deposition parameters of the coatings.

Sample	Ti-DLC mono		(Ti/Ti-DLC)2 multi		(Ti/Ti-DLC)4 multi	
	Transition layer	Ti-DLC	Transition layer or Ti sublayer	Ti-DLC sublayer	Transition layer or Ti sublayer	Ti-DLC sublayer
Deposition times (min)	5.5	54.5	10	20	5	10
Alternating numbers	0	0	2	2	4	4
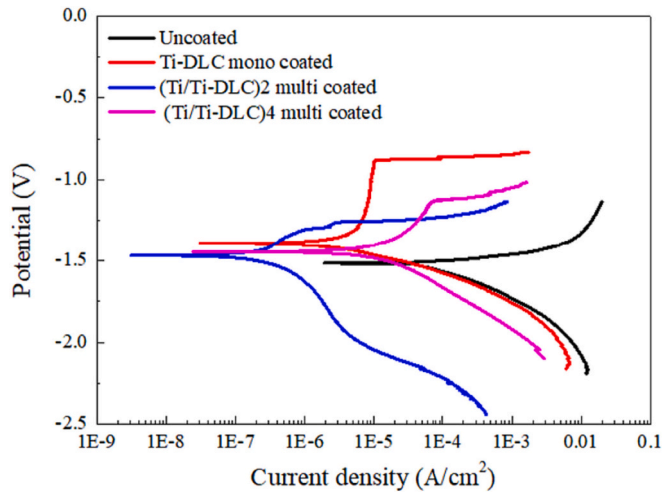
Fig. 1. Potentiodynamic polarization curves of the uncoated- and coated magnesium alloys.

2. Experiments

The substrates used for coating preparation were Si (100) sheets with a thickness of 0.5 mm and AZ31 magnesium alloy sheets with a thickness of 2 mm. The chemical composition of magnesium alloy is 3.1 wt% Al, 0.9 wt% Zn, 0.32 wt% Mn, 0.012 wt% Si, 0.0089 wt% Cu, 0.0021 wt% Fe, 0.0009 wt% Ni, and the rest is Mg. Magnesium alloy plates were firstly processed into 2 cm × 2 cm (length × width) by wire cutting, then grind with 400–2000 mesh SiC sandpaper and polished with 1 μm aluminum oxide alcohol suspension. Finally, clean the AZ31 magnesium alloys and Si plates in deionized water, followed by ultrasonic cleaning in acetone and ethanol for 5 min, respectively, and then dry.

The coating deposition equipment was a magnetic filtered cathode
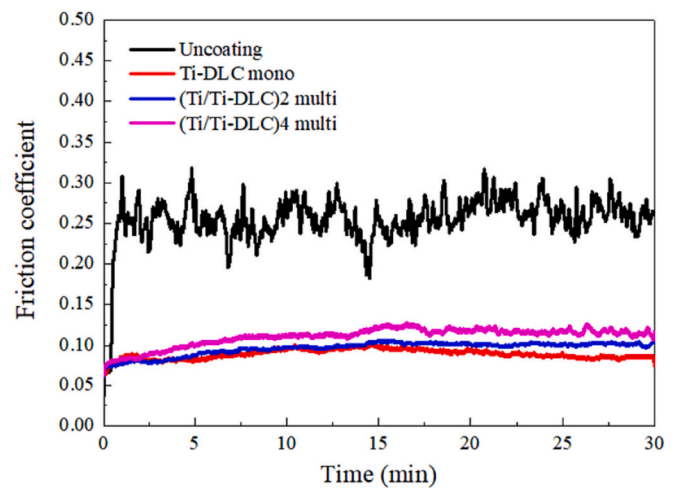
Fig. 3. Friction coefficient of the uncoated- and coated magnesium alloys.
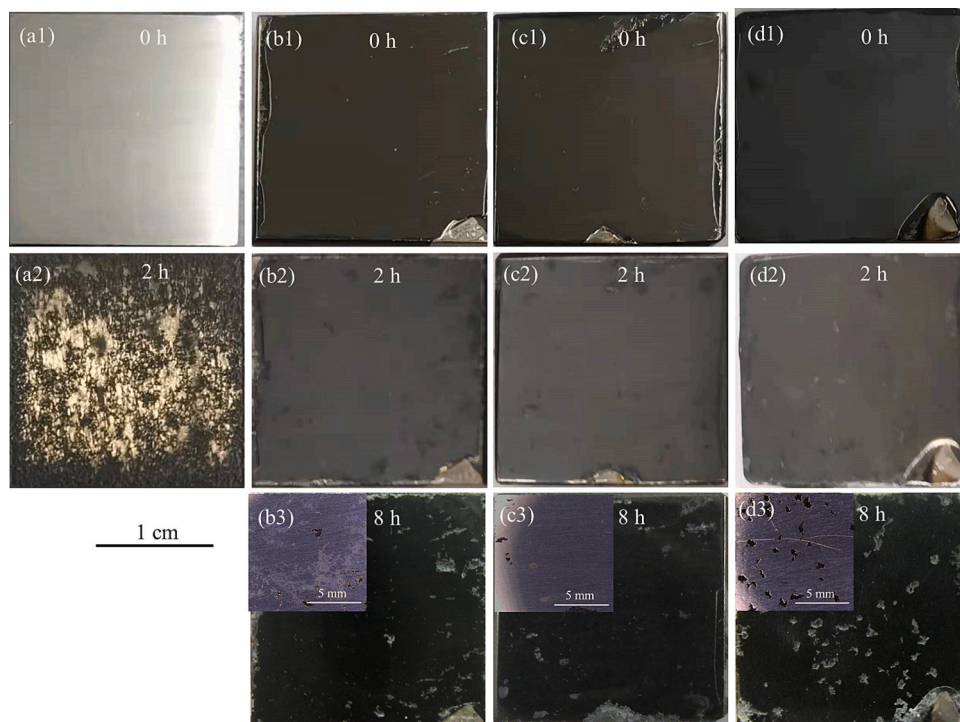
Fig. 2. Appearance of (a1-a2) uncoated-, (b1-b3) Ti-DLC mono coated-, (c1-c3) (Ti/Ti-DLC)2 multi coated-, and (d1-d3) (Ti/Ti-DLC)4 multi coated magnesium alloys after immersion for different times in 3.5 % NaCl solution.
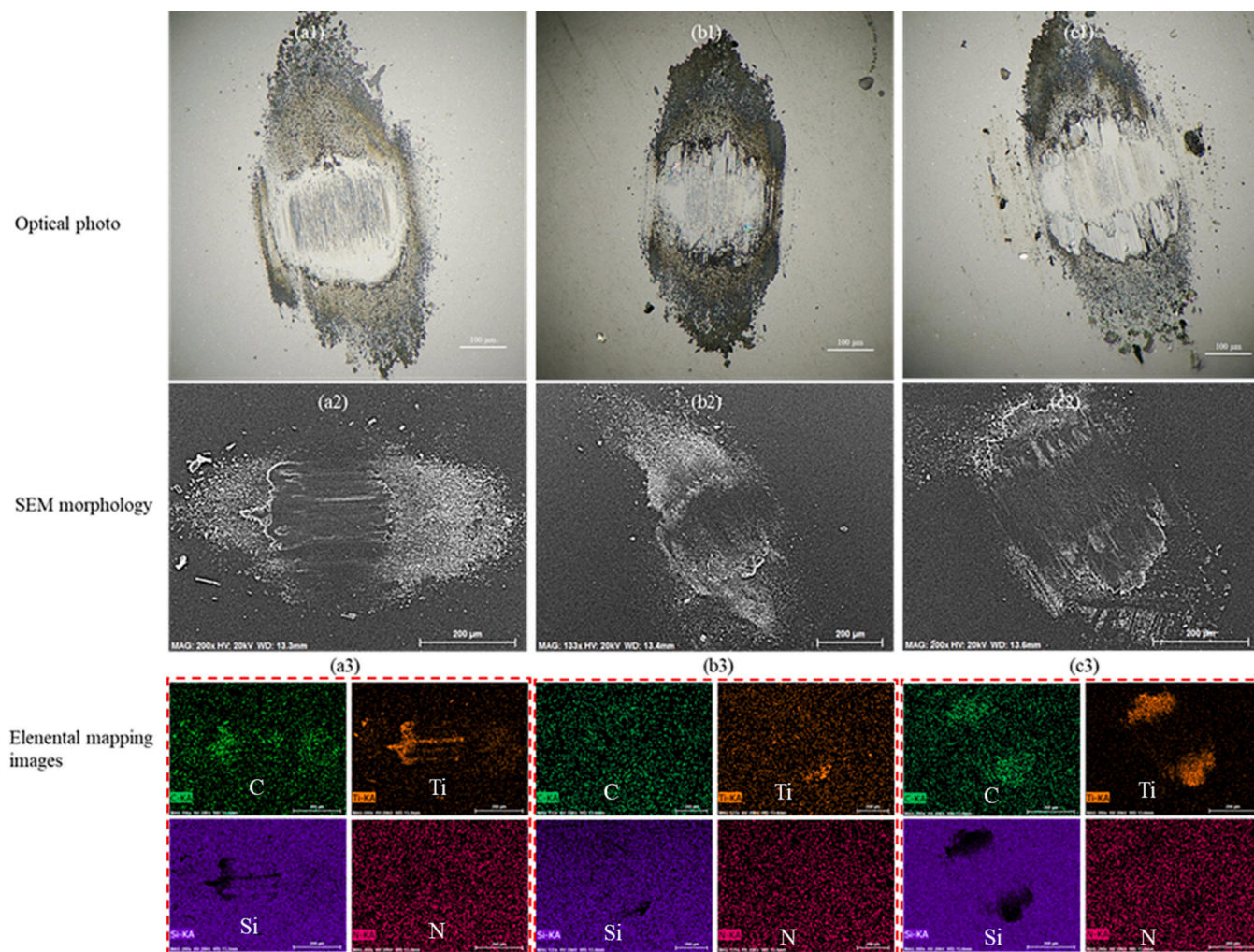
Fig. 4. (a1-c1) Optical photos, (a2-c2) SEM morphologies, and (a3-c3) elemental mapping images of the wear marks of the Si_3N_4 grinding balls against (a1-a3) Ti-DLC mono, (b1-b3) (Ti/Ti-DLC)2 multi, and (c1-c3) (Ti/Ti-DLC)4 multi films.

vacuum arc equipment developed by the School of Nuclear Science and Technology of Beijing Normal University. The 90° magnetic elbow was selected, and the sample table was maintained 45° to the magnetic elbow. Ti target with 99.99 % purity (ϕ 100 mm × 20 mm), and the reaction gas of C_2H_2 with 99.8 % purity were used. Firstly, substrate was sputtering cleaned at 800, 600, and 400 V substrate negative biases for 1 min, 2 min, and 1 min, respectively. A duty ratio of 40 %, an arc current of 85 A, and a magnetic field of 1.6 A were used. And then the transition layer and coating were deposited under - 80 V substrate bias. For the Ti doped DLC (Ti-DLC) monolayer and Ti-DLC sublayer of Ti/Ti-DLC multilayer films, the Ti plasma was accelerated and filtered through a magnetic bend, and finally mixed with the carbon plasma obtained from C_2H_2 ionization to form the film.

Before the deposition of film, a transition layer [11,20] was used to improve adhesion strength. The transition layer structure was composed of Ti adhesive layer/Ti-DLC insulating layer/Ti interlayer, with deposition times of 3 min, 30 s, and 2 min, respectively. The deposition parameters of Ti-DLC monolayer (Ti-DLC mono), (Ti/Ti-DLC)2 multilayer ((Ti/Ti-DLC)2 multi), and (Ti/Ti-DLC)4 multilayer ((Ti/Ti-DLC)4 multi) films were shown in Table 1. The total deposition time for all coatings was 60 min.

Corrosion resistance of the coating was evaluated by an electro-chemical workstation (PARSTAT2273) using a three-electrode system. The uncoated- or coated magnesium alloy was used as the working electrode, a platinum plate was used as the auxiliary electrode, and the

saturated calomel (SCE) was used as the reference electrode. The test was conducted in 3.5 wt% NaCl solution at room temperature with an 0.5 cm² exposed area for each sample. Soak the sample for 30–60 min to stabilize the open circuit potential, and then test the potentiodynamic polarization (PDP) curve of the sample. The test potential was set within the range of $-0.6 \sim +0.8$ V relative to the open circuit potential, and the scanning rate was 1 mV/s. Three parallel specimens were used for the test. After testing, the corrosion current density (i_{corr}) and corrosion potential (E_{corr}) of the sample were obtained by fitting the polarization curve using the Tafel extrapolation method.

Immersion test was also conducted to characterize corrosion resistance of the sample. The sample was sealed with a 2 cm × 2 cm exposed area for test. The immersion solution was 80 ml of 3.5 wt% NaCl solution (the ratio of solution volume to exposed area of coating was 20 ml/cm²) and experiment were conducted at room temperature. After immersion test, first cleaned the sample with deionized water and removed corrosion products from the sample surface with a soft brush. Then, the sample was cleaned using alcohol. Last, the sample was dried. The surface morphology of the corroded sample was photographed with a camera and a super depth of field micro 3D workstation (LY-WN-YH1000).

The MFT-EC4000 linear reciprocating friction and wear tester was used to test the dry friction and wear of the uncoated- and coated magnesium alloy samples. The test was carried out in the environment with room temperature and relative humidity of 30–40 % using a ϕ6 mm

Si_3N_4 ceramic grinding ball. A reciprocating frequency range of 1 Hz and 2 Hz, a wear scar length of 5 mm, and loads of 5 N and10 N was used for test. Each sample was tested for three times to ensure the reliability of the experimental data. The curve of wear depth and width was measured by a surface topography instrument (Talysurf5P-120). The wear rate W (mm^3/N· m) was calculated by eq. (1) at three different positions of the wear scar [21]:

$$W = V/(P \times L) \tag{1}$$

where V is the wear volume (mm^3), L is the slip distance (m), and P is the load (N).

The surface morphology and element composition of the sample after corrosion and wear were characterized by the ultra-depth of field micro 3D workstation and the Hitachi S-4800 scanning electron microscope (SEM) equipped with energy dispersive spectrometer (EDS).
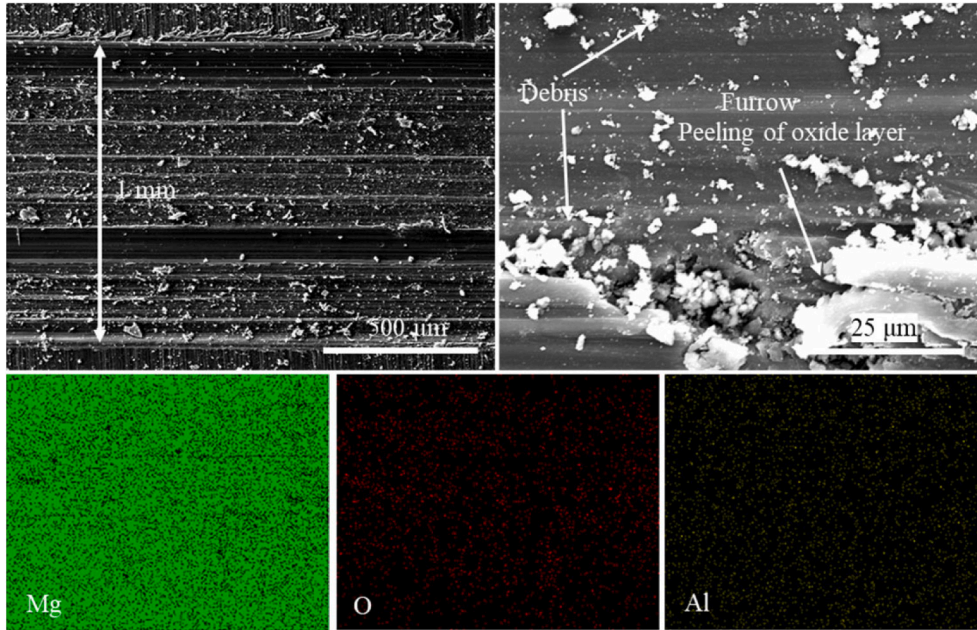
(a) Uncoated sample
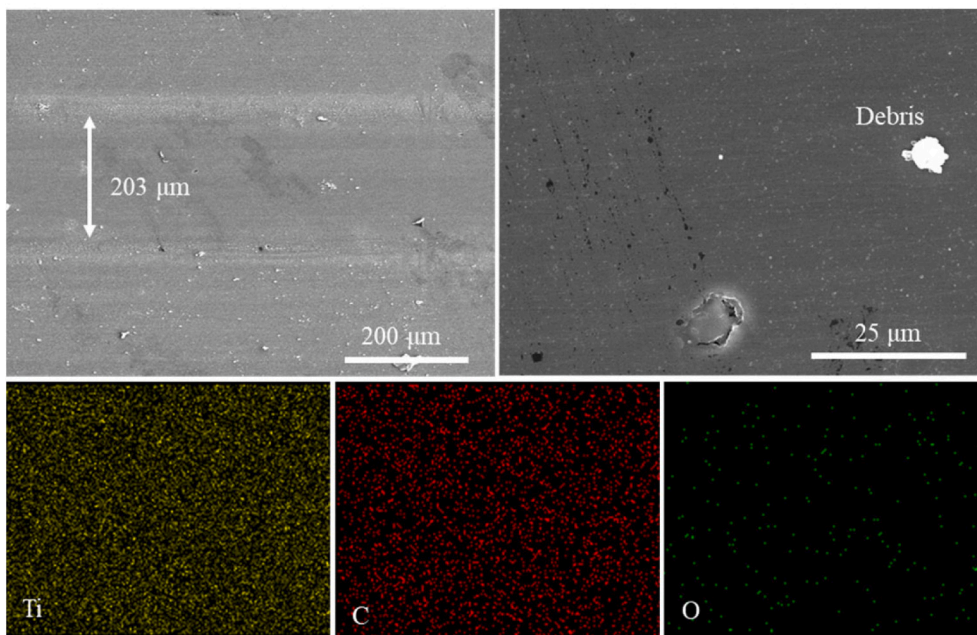
(b) Ti-DLC mono coated sample

Fig. 5. Surface SEM morphology at different magnification and elemental mapping images of wear marks of (a) uncoated-, (b) Ti-DLC mono coated-, (c) (Ti/Ti-DLC)2 multi coated-, and (d) (Ti/Ti-DLC)4 multi coated magnesium alloys.
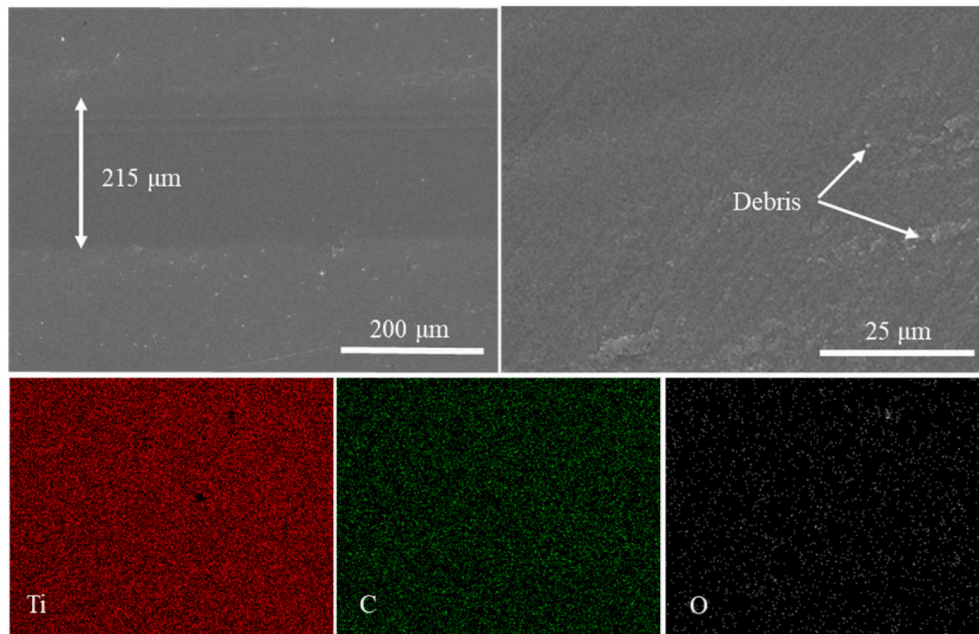
(c) (Ti/Ti-DLC)2 multi coated sample
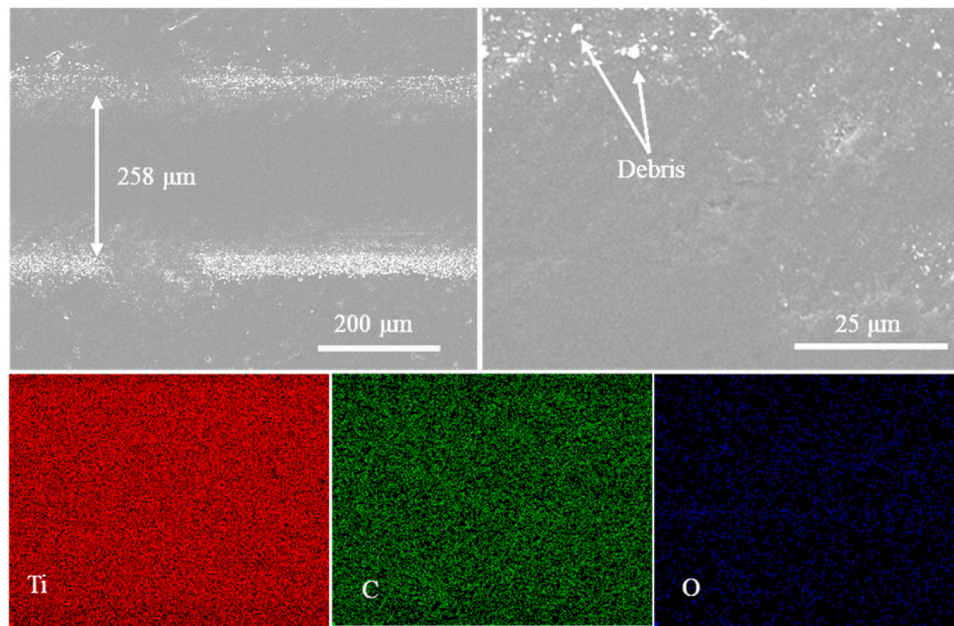
(d) (Ti/Ti-DLC)4 multi coated sample

Fig. 5. (*continued*).

3. Results and discussions

3.1. Corrosion resistance

Fig. 1 shows the PDP curves of the uncoated- and coated magnesium alloy samples. The corrosion current density and potential of the uncoated substrate was 3.13×10^{-4} A/cm^2 and -1.510 V, respectively. All coated samples showed lower corrosion current density and positive shift of potential. The corrosion current density of Ti-DLC mono coated sample was 1.64×10^{-6} A/cm^2, two orders of magnitude lower than uncoated magnesium alloy. And the corrosion potential was positively shifted to -1.394 V. The (Ti/Ti-DLC)2 multi coated sample showed the lowest corrosion current density of 1.16×10^{-7} A/cm^2, three orders of magnitude lower than uncoated magnesium alloy. The corrosion current density of (Ti/Ti-DLC)4 multi coated sample was 7.55×10^{-6} A/cm^2, between that of the Ti-DLC mono coated- and (Ti/Ti-DLC)2 multi coated samples. The result shows that all coatings improved corrosion resistance of the magnesium alloy, and the period of the multilayer film affected corrosion resistance of coating. The corrosion resistance of (Ti/Ti-DLC)2 multi film with a larger period was the best, while the corrosion resistance of the (Ti/Ti-DLC)4 multilayer film with a smaller period was even lower than that of the Ti-DLC mono film. Due to little difference in thickness, smaller period means more sublayers and thinner Ti and Ti-DLC sublayers of multilayer film, thus, the risk of corrosion
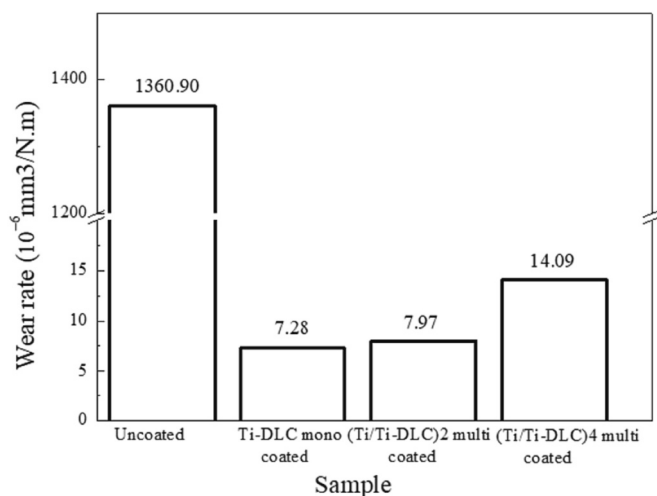
Fig. 6. Wear rates of the uncoated- and coated magnesium alloys under 5 N load and 1 HZ frequency.
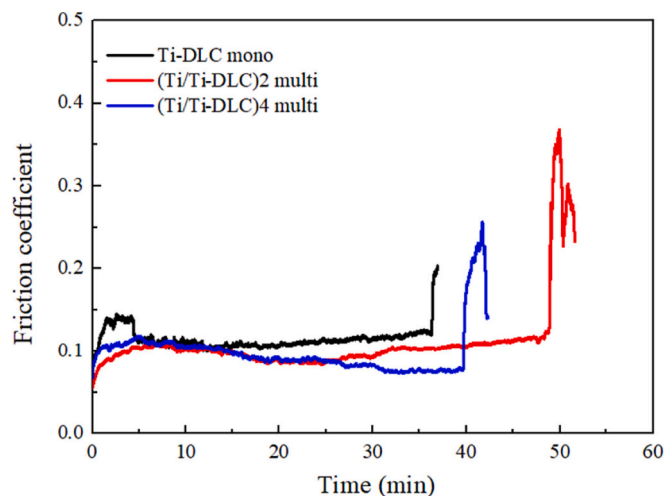
Fig. 7. Friction coefficient and wear life of the coatings under 10 N load and 2 Hz frequency.

medium penetrating the coating increased [14] and the corrosion resistance of coating decreased.

Fig. 2 shows the optical morphology of the uncoated- and coated magnesium alloy samples after immersion for 2 h and 8 h in 3.5 % NaCl solution. Before immersion, the surface of the uncoated- and coated samples was smooth and the coatings were intact and completely covered on the surface of the magnesium alloys. As well known, magnesium alloy had poor corrosion resistance. Once immersion began, the uncoated sample continuously generated a large number of bubbles due to release of H_2 caused by the corrosion of magnesium alloy. After 2 h, a large number of corrosion products were observed on the surface of sample. However, after soaking for 2 h, the coated samples were slight corroded and three coatings contained integrity. Three coatings provided good anti-corrosion protection for the magnesium alloys. During immersion test, all coated samples locally generated a few bubbles, indicating that the corrosion medium penetrated into the magnesium alloy substrate along the pinhole defects in coating. After immersion for 8 h, all coated samples underwent pitting and local corrosion. The corrosion area of the samples, in descending order, was (Ti/Ti-DLC)4 multi coated sample, Ti-DLC mono coated sample, and (Ti/Ti-DLC)2 multi coated sample. This result indicates that the (Ti/Ti-DLC)2 multi coated sample had the best corrosion resistance, followed by Ti-DLC

mono coated sample, and (Ti/Ti-DLC)4 multi coated sample had the worst corrosion resistance. This result is consistent with the electrochemical test results.

Usually, metal transition layer can improve the bonding strength of film but increase the risk of galvanic corrosion between the coating and magnesium alloy substrate [22]. The Ti-DLC mono film showed good corrosion resistance is due to: (1) poor conductivity of Ti-DLC film; (2) few defects in coating with dense amorphous structure [14]; (3) the transition layer improved the adhesion between the coating and substrate, prevented the coating from peeling off during the corrosion process; (4) the Ti-DLC insulating layer in the transition layer delayed corrosion of magnesium alloy. According to the schematic diagram of the transition layer in Fig. 1 in Part 1, the transition layer was composed of the Ti interlayer/Ti-DLC insulation layer/Ti adhesion layer (along the outer layer to substrate direction). When the corrosion solution reached the interface of substrate/transition layer through coating defects, galvanic corrosion of magnesium alloy substrate/Ti adhesion layer and electrochemical corrosion of the magnesium alloy occurred, and the corrosion products were stacked between the Ti adhesion layer and magnesium alloy. Furthermore, the Ti-DLC insulation layer hindered the diffusion of galvanic corrosion to the coating. As a result, corrosion process was obstructed.

In addition to the above reasons, the best corrosion resistance of (Ti/Ti-DLC)2 multi film was related to the following factors: (1) pinhole defects in coating were deflected by multi-interface effect of the multilayer, resulting in the corrosion channels were hindered and prolonged. This phenomenon is similar to the deflection effect in multilayer toughening mechanism [23]; (2) the lowest internal stress and highest toughness of film inhibited propagation of pinhole defects during corrosion process; (3) the good deformation coordination of the multilayer film ensured a good combination between the coating and substrate during corrosion process [16], preventing the peeling failure of the coating. However, the corrosion resistance of (Ti/Ti-DLC)4 multi film was worse than that of (Ti/Ti-DLC)2 multi and Ti-DLC mono films. That is because that the thin Ti sublayers (about 80 nm thick) in the multilayer increased the risk of corrosion media penetrating the multilayer interface [14], resulting in more corrosion channels were formed.

3.2. Wear resistance

Fig. 3 shows coefficient of friction (COF) of the uncoated- and coated magnesium alloy samples against Si_3N_4 balls under a load of 5 N. After 1 min, the uncoated magnesium alloy entered a stationary friction period, with a coefficient of friction fluctuating around 0.25. After coating, the friction coefficient was decreased significantly. For all coated samples, there was little difference in COF during the first 2 min, and then it gradually increased. After 14 min, for the (Ti/Ti-DLC)2 multi coated- and (Ti/Ti-DLC)4 multi coated specimen, the friction coefficient kept the relatively stable values of around 0.10 and 0.12 until the end of friction, respectively. However, the COF of Ti-DLC mono coated sample gradually decreased from 0.096 to 0.086. The friction coefficients of three coatings in descending order was Ti-DLC mono, (Ti/Ti-DLC)2 multi, and (Ti/Ti-DLC)4 multi films. Compared with the Ti-DLC mono film, the Ti/Ti-DLC multi films exhibited higher COF values due to the involvement of the damaged Ti sublayer in the friction process. Compared with the (Ti/Ti-DLC)2 multi film, the (Ti/Ti-DLC)4 multi film had a smaller period, i.e., a thinner top Ti-DLC sublayer. During the friction process, after this thinner top Ti-DLC sublayer was worn, the Ti sublayer participated in wear. Due to the lower hardness of Ti sublayer, wear depth would be deeper and a greater amount of Ti would participate in wear, resulting in a higher friction coefficient.

All coatings have low COF value below 0.15, exhibiting excellent lubricity. EDS spectrum analysis and morphology observation were conducted on the wear scars of Si_3N_4 grinding balls and the worn surface of the coated samples, as shown in Figs. 4 and 5, respectively. After friction, the smooth wear product was adhered to the surface of Si_3N_4
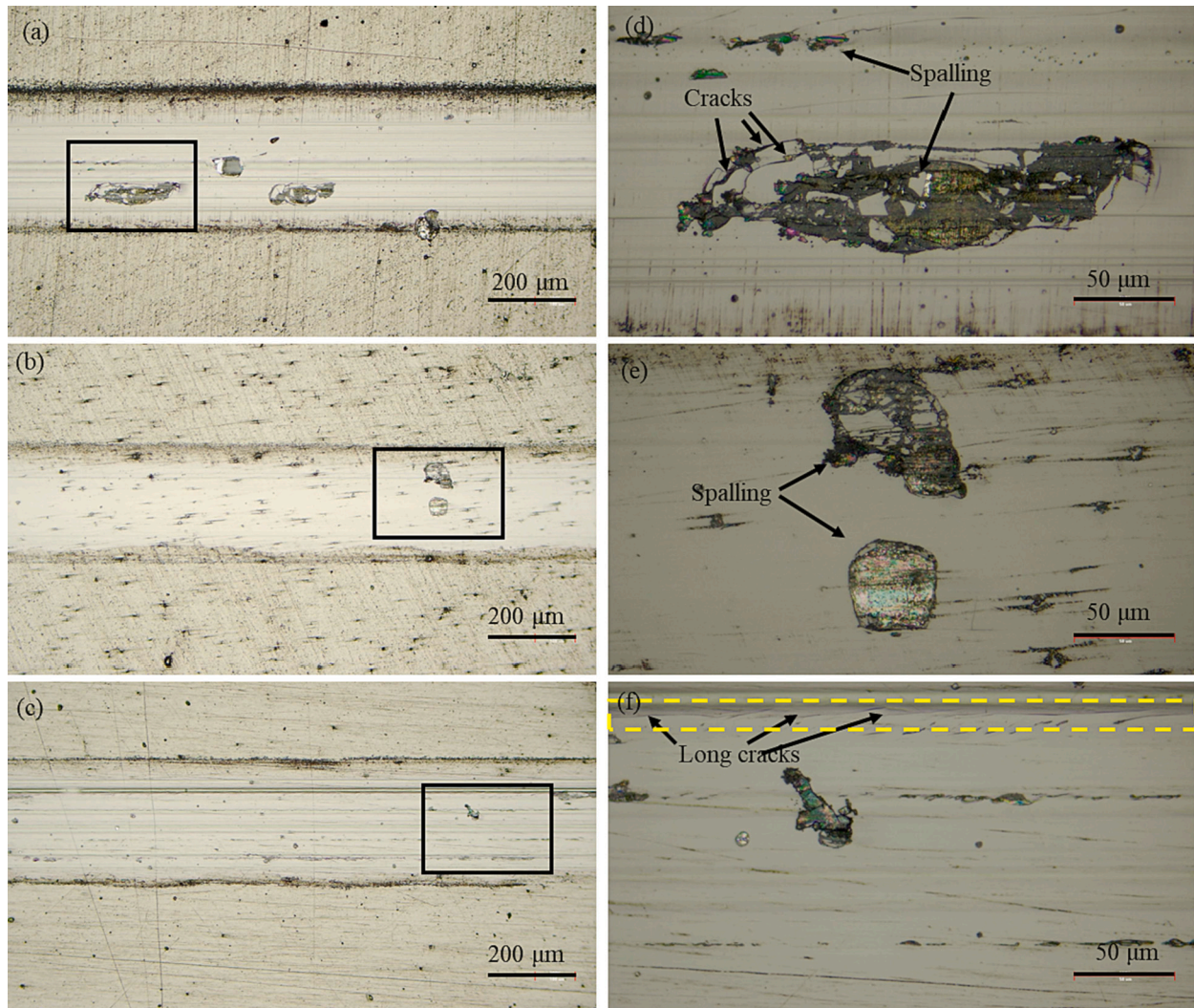
Fig. 8. Optical photos of the wear marks of (a, d) Ti-DLC mono coated-, (b, e) (Ti/Ti-DLC)2 multi coated-, and (c, f) (Ti/Ti-DLC)4 multi coated magnesium alloys at different magnification after friction for 10 min.

grinding balls (Fig. 4 a1-c1 and a2-c2). For each Si$_3$N$_4$ grinding ball, a comet like black transfer layer (Fig. 4 a1-c1) was observed on both sides of the wear scar. The elemental mapping images showed that Ti and C elements were enriched in the wear product (Fig. 4 a3-c3). Excellent lubricity of coatings with low COF values is attributed to: (1) the low shear stress between smooth wear product layer with rich C and the coated sample reduced friction coefficient [24]; (2) the high I_D/I_G ratios (1.89–4.83) (Fig. 3 in Part 1) of coatings meant that the high content of sp^2 in coatings; (3) the transformation of transfer film on the grinding ball increased the content of sp^2 and formed a graphite interface layer that was easy to slip between the friction interfaces, resulting in a decrease in the friction coefficient [25].

As shown in Fig. 5 a, for the uncoated magnesium alloy substrate, wear width was about 1 mm. Deep furrows and a large amount of wear debris were seen within the wear scar due to the severe wear, and some debris was transferred to the outer side of the wear mark with the movement of the grinding ball. Due to the oxidization of debris occurred during wear process, the EDS results show that O element uniformly distributed inside and outside the wear scar. In addition, the obvious oxide layer peeling was observed within the wear mark.

For the Ti-DLC mono coated-, (Ti/Ti-DLC)2 multi coated-, and (Ti/Ti-DLC)4 multi coated samples, the number of debris were significantly reduced, and the wear width was significantly decreased to 203, 215, 258 μm, respectively. The surfaces of coatings were smooth and flat

without obvious worn (Fig. 5 b-d). It indicated that all coatings provided excellent wear protection for magnesium alloys. In addition, the debris was almost not distributed within the wear marks, but accumulated along the friction direction on the outer side of wear marks [26]. This is because the transfer film (or thin graphite layer) was formed on the grinding ball (Fig. 4), resulting in the friction between the coating and grinding ball reduced. Therefore, the debris generated during early wear was gradually transferred beyond the wear marks with the grinding ball moving.

For all Ti-DLC coated samples, there was no difference in the concentration of C, and Ti elements inside and outside the wear scar, which proves that the coatings were not invalid. For the Ti-DLC mono film, the low content of O element means that because Ti element existed in TiC nanocrystals wrapped by amorphous carbon parent phase, no obvious oxidation occurred during the wear process. However, compared to the Ti-DLC mono coated sample, the Ti/Ti-DLC multi coated samples showed larger wear width, indicating greater wear depth. Furthermore, the (Ti/Ti-DLC)2 multi film exhibited a smaller wear width than the (Ti/Ti-DLC)4 multilayer (Figs. 5 c and d), which is attributed to its higher hardness and thicker top Ti-DLC sublayer.

As shown in Fig. 6, for the uncoated sample, the wear rate calculated by Formula (1) was 1360.9 × 10^{-6} mm^3/N· m. However, the wear rate of Ti-DLC mono coated-, (Ti/Ti-DLC)2 multi coated, and (Ti/Ti-DLC)4 multi coated magnesium alloys was 7.28 × 10^{-6} mm^3/N· m, 7.97 ×
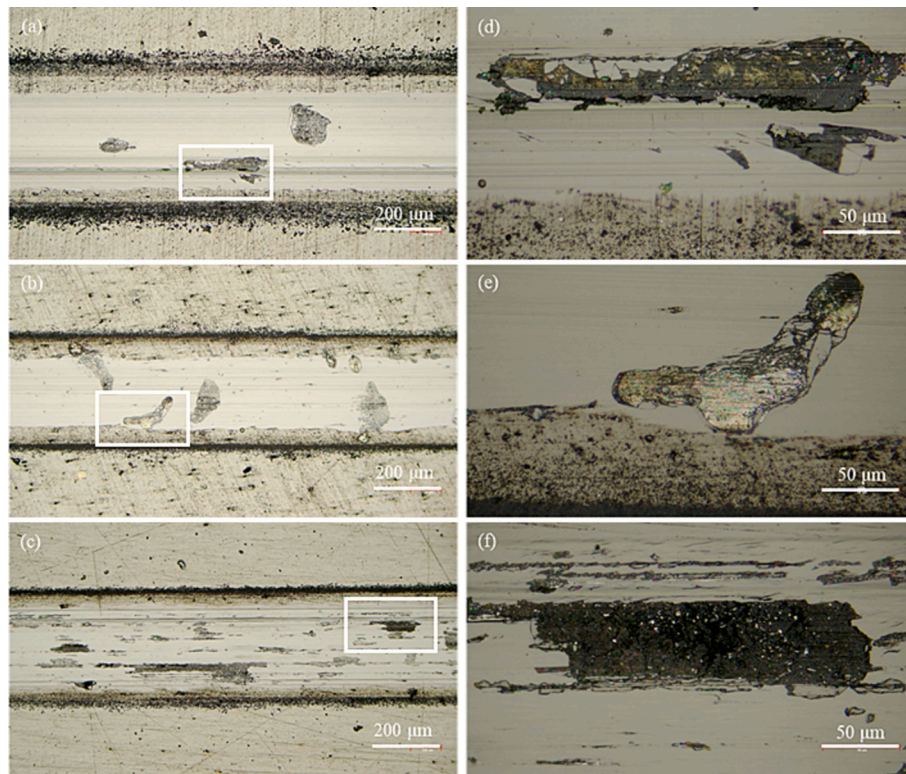
Fig. 9. Optical photos of the wear marks of (a, d) Ti-DLC mono coated-, (b, e) (Ti/Ti-DLC)2 multi coated-, and (c, f) (Ti/Ti-DLC)4 multi coated magnesium alloys at different magnification after friction for 30 min.

10^{-6} mm^3/N· m, and 14.09 × 10^{-6} mm^3/N· m, respectively, nearly 2 to 3 orders of magnitude lower than that of the uncoated sample. That is because, as mentioned earlier, metal doped DLC coating has good wear resistance due to its lubrication effect. In addition, all coatings had good toughness and much higher hardness than the magnesium alloy (Table 3 in Part 1). Therefore, all coatings provided good wear protection for magnesium alloy. In addition, under 5 N load, the Ti-DLC mono film showed a lower wear rate and more excellent wear resistance than the Ti/Ti-DLC multilayers due to its higher hardness and good toughness (fracture toughness >3 [27]). Furthermore, compared with the (Ti/Ti-DLC)4 multi film, the wear rate of (Ti/Ti-DLC)2 multi film was lower due to its higher hardness and toughness.

Our previous study [17] showed that, due to its higher toughness, better deformation coordination of the substrate/coating, and layer by layer wear mechanism, crack initiation and propagation during the wear process are effectively suppressed, and the coating is less prone to peeling off. Multilayer film usually exhibits better wear resistance than monolayer film. According to the above results, under 5 N load, the Ti-DLC monolayer had the most wear resistance with the lowest friction coefficient and wear rate. Why? Due to the Ti-DLC film has good lubrication and wear resistance, under 5 N load, mainly the top Ti-DLC sublayer of multilayer films participated in wear (Fig. 5). Therefore, an assumption is the advantages of good toughness of multilayer film and good deformation coordination between coating and substrate [17] had not yet been fully exploited under short friction times or low loads.

To further elucidate the role of toughness in improving wear resistance, the wear life of coatings was tested under 10 N load and 2 HZ frequency. The total friction time before a significant change in friction coefficient occurs due to coating failure was considered the wear life of the coating [17]. The curve of friction coefficient variation with time was shown in Fig. 7. The results show that the wear life of Ti-DLC mono, (Ti/Ti-DLC)2 multi, and (Ti/Ti-DLC)4 multi films was 36.5, 49.5 min, and 42 min, respectively. The Ti-DLC multilayer films showed longer wear life than the Ti-DLC monolayer film.

Figs. 8 and 9 show the optical photos of wear scars of the coated samples under 10 N load and 2 HZ frequency for 10 min and 30 min friction, respectively. After 10 min friction, the Ti-DLC monolayer film peeled off locally in large areas (Fig. 8 a), and there were numerous cracks in the peeled area (Fig. 8 d). This phenomenon can be explained as: on the one hand, although the Ti-DLC monolayer film could withstand large 10 N load of friction, the soft magnesium alloy substrate could not provide sufficient support, leading to the failure of the coating due to the collapse of the substrate. And on the other hand, under the friction load, with the increase of wear time, the load transmitted to the magnesium alloy substrate caused plastic deformation, which is much greater than the deformation of the hard Ti-DLC coating. This disrupted the bonding between the coating and the magnesium alloy substrate, leading to the failure of the coating due to the loss of substrate support. Therefore, the Ti-DLC monolayer failed after friction for 36.5 min. However, for the Ti/Ti-DLC multi films, due to their better toughness and good deformation compatibility between the coating and substrate, the area of local peeling (Fig. 8 b, c) of the coating was reduced, and the visible cracks (Fig. 8 e, f) in the peeling area were reduced. Also, the narrower wear width (Fig. 8 b, c) indicates that the Ti/Ti-DLC multi films had better wear resistance than the Ti-DLC mono film. In addition, although the (Ti/Ti-DLC)4 multi film had a smaller peeling area, there were some long cracks (yellow dashed rectangular box in Fig. 8 f) along the length direction of wear scar, which infers that as the further increase of wear time, the coating would soon fail.

After friction for 30 min, as shown in Fig. 9, the local peeling area of all coatings increased. For the Ti-DLC mono film, a large amount of wear debris accumulated on both sides of the wear track and the width of the wear scar was the largest. This means the Ti-DLC mono film experienced severe wear. Whereas, the wear width of the (Ti/Ti-DLC)2 multi and (Ti/Ti-DLC)4 multi films was lower than that of the Ti-DLC mono film. Thus, under 10 N load, the Ti/Ti-DLC multi films had better wear resistance than the Ti-DLC mono film. Furthermore, the difference of the wear width of the (Ti/Ti-DLC)2 multi and (Ti/Ti-DLC)4 multi films was small.

This result indicates that after friction for >10 min, compared to (Ti/Ti-DLC)2 multi film, the degree of accelerated wear of (Ti/Ti-DLC)4 multi film was more significant than that of (Ti/Ti-DLC)2 multi film. This is not difficult to understand because after friction for >10 min, the long cracks previously formed in the (Ti/Ti-DLC)4 multi film rapidly propagated and expanded into flakes, leading to severe spalling of the coating. Then, the peeled wear debris were partially retained in the wear trajectory to accelerate wear. Thus, the wear life of the (Ti/Ti-DLC)4 multi film was lower than that of the (Ti/Ti-DLC)2 multilayer film.

4. Conclusions

Three coatings, namely Ti-DLC monolayer, (Ti/Ti-DLC)2 and (Ti/Ti-DLC)4 multilayer films were prepared on the magnesium alloys using magnetic filtered cathode vacuum arc technology. Corrosion resistance and wear resistance, as well as corrosion and wear resistance mechanisms of the coatings were investigated, and the following conclusions were drawn:

(1) All coatings exhibited good corrosion and wear resistance. Corrosion current density of the Ti-DLC mono coated-, (Ti/Ti-DLC)2 multi coated, and (Ti/Ti-DLC)4 multi coated samples was 2–3 orders of magnitude lower than that of the uncoated magnesium alloy. And the (Ti/Ti-DLC)2 multilayer coated sample showed a lowest corrosion current density of 1.16×10^{-7} A/cm^2. Under a load of 5 N and a frequency of 1 HZ, the friction coefficient of all coatings was below 0.12, the wear rate was 2–3 orders of magnitude lower than that of uncoated the magnesium alloy, and the Ti-DLC monolayer had the lowest wear rate of 7.28×10^{-6} mm^3/N· m. However, under a load of 10 N and a frequency of 2 HZ, compared with the Ti-DLC monolayer, the Ti/Ti-DLC multilayer films showed a longer wear life, and the (Ti/Ti-DLC)2 multilayer obtained the longest wear life of 49.5 min, 36 % higher than the Ti-DLC monolayer.

(2) The Ti-DLC monolayer film had excellent corrosion resistance is due to the Ti-DLC insulation layer in the transition layer, dense amorphous structure, and good adhesion between the Ti-DLC monolayer film and the substrate. The reasons for the further improvement of corrosion resistance of Ti/Ti-DLC multilayer films is attributed to the deflection effect of pinhole defects and good deformation coordination between the multilayer film and substrate during corrosion process.

(3) Under 5 N load, the most excellent wear resistance of Ti-DLC monolayer film is attributed to highest hardness and good lubricity by forming a transfer film on the grinding ball. However, under 10 N load, comparing to the Ti-DLC monolayer film, the Ti/Ti-DLC multilayer films gained longer wear life due to their better toughness and deformation coordination between coating and substrates. In indicates that, under the larger load, toughness of coating and deformation coordination between coating and substrate played an important role in improving wear resistance.

Declaration of competing interest

The authors declare that they have no known competing financial interests or personal relationships that could have appeared to influence the work reported in this paper.

Data availability

No data was used for the research described in the article.

References

[1] J.E. Gray, B. Luan, Protective coatings on magnesium and its alloys — a critical review, J. Alloys Compd. 33 (26) (2002) 88–113.

[2] M. Esmaily, J.E. Svensson, S. Fajardo, N. Birbilis, G.S. Frankel, S. Virtanen, R. Arrabal, S. Thomas, L.G. Johansson, Fundamentals and advances in magnesium alloy corrosion, Prog. Mater. Sci. 89 (2017) 92–193.

[3] Y. Ren, Study of bio-corrosion of pure magnesium, Acta Metall. Sin. 41 (11) (2005) 1228–1232.

[4] G. Song, Control of biodegradation of biocompatable magnesium alloys, Corros. Sci. 49 (4) (2007) 1696–1701.

[5] E. Zhang, L. Yang, J. Xu, H. Chen, Microstructure, mechanical properties and bio-corrosion properties of mg-Si(-ca, Zn) alloy for biomedical application, Acta Biomater. 6 (5) (2010) 1756–1762.

[6] G. Reiners, M. Griepentrog, Hard coatings on magnesium alloys by sputter deposition using a pulsed d.c. bias voltage, Surf. Coat. Technol. 76–77 (1995) 809–814.

[7] Y. Dong, T. Wang, Y. Xu, Y. Guo, G. Li, J. Lian, A polydopamine-based calcium phosphate/graphene oxide composite coating on magnesium alloy to improve corrosion resistance and biocompatibility for biomedical applications, Materialia 21 (2022), 101315.

[8] L. Pezzato, V. Angelini, K. Brunelli, C. Martini, M. DabalÀ, Tribological and corrosion behavior of PEO coatings with graphite nanoparticles on AZ91 and AZ80 magnesium alloys, Trans. Nonferrous Metals Soc. China 28 (2) (2018) 259–272.

[9] X. Liu, Q. Yang, Z. Li, W. Yuan, Y. Zheng, Z. Cui, X. Yang, K.W.K. Yeung, S. Wu, A combined coating strategy based on atomic layer deposition for enhancement of corrosion resistance of AZ31 magnesium alloy, Appl. Surf. Sci. 434 (2018) 1101–1111.

[10] M. Cichomski, B. Burnat, M. Prowizor, A. Jedrzejczak, D. Batory, I. Piwoński, W. Kozłowski, W. Szymanski, M.J.T.I. Dudek, Tribological and corrosive investigations of perfluoro and alkylphosphonic self-assembled monolayers on Ti incorporated carbon coatings 130, 2019, pp. 359–365.

[11] H. Cao, X. Ye, H. Li, F. Qi, Q. Wang, X. Ouyang, N. Zhao, B. Liao, Microstructure, mechanical and tribological properties of multilayer Ti-DLC thick films on Al alloys by filtered cathodic vacuum arc technology, Mater. Des. 198 (2021), 109320.

[12] I. Masami, N. Setsuo, S. Tsutomu, C. Junho, Improvement of corrosion protection property of Mg-alloy by DLC and Si–DLC coatings with PBII technique and multi-target DC–RF magnetron sputtering, Nuclear Instruments & Methods in Physics Research 267 (8–9) (2009) 1675–1679.

[13] W. Dai, A. Wang, Deposition and properties of Al-containing diamond-like carbon films by a hybrid ion beam source, J. Alloys Compd. 509 (2011) 4626–4631.

[14] D. Zhang, Z. Qi, B. Wei, Z. Wu, Z. Wang, Anticorrosive yet conductive Hf/Si3N4 multilayer coatings on AZ91D magnesium alloy by magnetron sputtering, Surf. Coat. Technol. 309 (2017) 12–20.

[15] L.H. Tian, E.Q. Liu, A.L. Fan, L. Qin, D.X. Liu, B. Tang, J.D. Pan, Effect of TiN/CrN multilayer coating by cathodic arc deposition on Wear and corrosion Behaviours of AZ91D magnesium alloy, Mater. Sci. Forum (2009) 870–873.

[16] W. Xie, Y. Zhao, S. Chen, B. Liao, S. Zhang, Q. Hua, G. He, Corrosion resistance of AlN monolayer and Al/AlN multilayer deposited by filtered cathodic vacuum arc, Thin Solid Films (2023) 139762.

[17] W. Xie, Y. Zhao, B. Liao, S. Wang, S. Zhang, Comparative tribological behavior of TiN monolayer and Ti/TiN multilayers on AZ31 magnesium alloys, Surf. Coat. Technol. 441 (2022) 12580.

[18] Wenling Xie, L. Bin, Z. Sam, Roads toward Surface Protection of Magnesium Alloys, CRC Press, United States, 2021.

[19] W. Xie, Y. Zhao, B. Liao, P. Pang, D. Wuu, S. Zhang, Al–AlN composite coatings on AZ31 magnesium alloy for surface hardening and corrosion resistance, Vacuum 188 (2021), 110146.

[20] R. Ali, M. Sebastiani, E. Bemporad, Influence of Ti–TiN multilayer PVD-coatings design on residual stresses and adhesion, Mater. Des. 75 (2015) 47–56.

[21] H.N. Vatan, R. Ebrahimi-kahrizsangi, M. Kasiri-asgarani, Structural, tribological and electrochemical behavior of SiC nanocomposite oxide coatings fabricated by plasma electrolytic oxidation (PEO) on AZ31 magnesium alloy, J. Alloys Compd. 683 (2016) 241–255.

[22] D. Zhang, B. Wei, Z. Wu, Z. Qi, Z. Wang, A comparative study on the corrosion behaviour of Al, Ti, Zr and Hf metallic coatings deposited on AZ91D magnesium alloys, Surf. Coat. Technol. 303 (2016) 94–102.

[23] L. Feike, S. Yufan, P. Chenrui, Q. Bin, L. Jing, S. Deen, Microstructure evolution and corrosion resistance of multi interfaces Al-TiAlN nanocomposite films on AZ91D magnesium alloy, Surf. Coat. Technol. 357 (2019) 83–92.

[24] X.J. Cui, C.M. Ning, L.L. Shang, G.A. Zhang, X.Q. Liu, Structure and anticorrosion, friction, and Wear characteristics of pure diamond-like carbon (DLC), Cr-DLC, and Cr-H-DLC films on AZ91D mg alloy, J. Mater. Eng. Perform. 28 (2019) 1213–1225.

[25] F. Zhao, H. Li, L. Ji, Y. Wang, H. Zhou, J. Chen, Ti-DLC films with superior friction performance, Diam. Relat. Mater. 19 (4) (2010) 342–349.

[26] W. Dai, G.S. Wu, A.Y. Wang, Preparation, characterization and properties of Cr-incorporated DLC films on magnesium alloy, Diam. Relat. Mater. 19 (10) (2010) 1307–1315.

[27] Y.X. Ou, X.P. Ouyang, B. Liao, X. Zhang, S. Zhang, Hard yet tough CrN/Si_3N_4 multilayer coatings deposited by the combined deep oscillation magnetron sputtering and pulsed dc magnetron sputtering, Appl. Surf. Sci. 502 (2020) 144168.1–144168.9.